

WEAKLY BARRED EARLY-TYPE RINGED GALAXIES. IV. THE DOUBLE-RINGED S0⁺ GALAXY NGC 7702

R. BUTA¹

Department of Physics and Astronomy, University of Alabama, Box 870324, Tuscaloosa, AL 35487

Received 1990 July 5; accepted 1990 August 31

ABSTRACT

The southern galaxy NGC 7702 is an interesting example of a late S0 galaxy showing a high-contrast inner ring surrounding a bright bulge, with no conventional bar crossing the ring as in typical SB(r)-type galaxies. It also has a low-contrast outer ring whose peak surface brightness is only ~6% of the night sky brightness in blue light. This paper presents *UBVRI* CCD surface photometry of NGC 7702 as a mean of evaluating its structure and properties with a view toward understanding the origin of the rings and how they relate to problems of internal dynamics. The photometry reveals the typically complex structure of a double-ringed galaxy both in terms of profile properties and color distribution. The inner ring is a subtle blue enhancement compared to its surroundings, and in addition shows azimuthal variations in color and surface brightness, due in part to internal extinction and tilt and also probably to an intrinsically oval shape. Long-exposure spectra taken along the major and minor axes reveal mainly a continuous spectrum in the inner ring region, and average colors are consistent with a feature that may have experienced a burst of star formation less than 2×10^9 yr ago which abruptly cut off after 10^7 yr. The bulge of the galaxy shows a distinctive oval shape and may be characterized as a nuclear bar ~1 kpc in diameter; it is reminiscent of the triaxial bulges observed in some SB galaxies. Fourier analysis also suggests that the inner ring lies near the boundary of an oval distortion or lens. The nonaxisymmetric component (excluding the nuclear oval) contributes about 14% of the total B band luminosity.

Although NGC 7702 is not a conventional barred galaxy, the two rings possess many properties in common with barred galaxy rings. It is possible that NGC 7702 once had a stronger, more important bar which lasted long enough to generate the rings but which is now mostly dissolved. The triaxial bulge may be a relic of such a past feature.

Subject headings: galaxies: individual (NGC 7702) — galaxies: photometry — galaxies: structure

1. INTRODUCTION

In the first paper of this series, it was stated that some of the most spectacular examples of ring phenomena in the sky are observed in weakly barred or nonbarred early-type disk galaxies. The southern S0⁺ galaxy NGC 7702 exemplifies this fact more than any other: it possesses an exceptionally conspicuous inner ring, but is sufficiently “nonbarred” that on direct plates it actually resembles the planet Saturn (see, for example, de Vaucouleurs & Buta 1980a). NGC 7702 is a particularly distinctive example because of the high contrast of its inner ring and the extreme faintness of its outer ring. It is an interesting problem to try and understand how the rings formed in a galaxy like this, because numerical simulations have suggested that both a nonaxisymmetric potential and gas are essential ingredients for ring formation in disk galaxies. NGC 7702 seems to contradict this scenario because of its early type and because its rings are largely stellar; it is not obvious how such purely stellar rings can have formed in the absence of a significant bar or barlike structure. This is the main issue being addressed in this series, which has thus far covered three examples: NGC 3081 (Buta 1990a, Paper I), NGC 7187 (Buta 1990b, Paper II), and NGC 7020 (Buta 1990c, Paper III).

Galaxies like NGC 7702 are also important because they may provide clues to the nature of the S0 phenomenon in

general (i.e., the “burnt-out” or “stripped” spiral theories vs. the intrinsic formation theory; see Dressler 1984; van Driel 1987; Gregg 1989a, b). Rings link spirals and S0s together in a manner which suggests secular evolution processes are important. In addition, the study of ringed early-type galaxies is another essential step in the attempt to understand what physical properties underlie revised Hubble classifications of galaxies (see, e.g., Kormendy 1979).

In this final paper of the series, I present *UBVRI* CCD surface photometry and *BV* photographic surface photometry of NGC 7702 as a means of evaluating its basic structure and properties. Though it is not a typical example, it is a fitting one to end the series with because it is perhaps the most enigmatic of the four which I have considered. Section 2 describes the observations, while § 3 discusses the morphology and group membership. An analysis of the data is presented in § 4, with a discussion in § 5. Conclusions are presented in § 6.

2. OBSERVATIONS

The CCD observations of NGC 7702 were made with the same equipment (3.9 m Anglo-Australian Telescope, RCA chip) and filters (Johnson *UBV*; Cousins *RI*) as used for the previous three galaxies in the series. To ensure that the field of the chip would have an adequate amount of sky, the CCD was oriented with its long axis north-south, or nearly along the galaxy minor axis. This caused the galaxy to overflow the field of view ($2'.6 \times 4'.2$) of the CCD by a small amount.

In addition to the CCD images, two prime focus plates obtained in 1981 July with the 4 m telescope of Cerro Tololo

¹ Visiting Astronomer, Cerro Tololo Inter-American Observatory, National Optical Astronomy Observatories, which is operated by the Association of Universities for Research in Astronomy, Inc. (AURA), under cooperative agreement with the National Science Foundation.

TABLE 1A
OBSERVING LOG OF CCD IMAGES

Filter	Sky (ADU)	Exposure (s)	$\mu_s(\text{Ap.})^a$ (mag s ⁻²)	$\mu_s(\text{S.S.})^b$ (mag s ⁻²)	Seeing (FWHM)
U	130.5	1000	21.71	21.68	1".70
B	127.5	350	22.44	22.41	1.44
V	180.0	225	21.49	21.45	1.57
R	175.9	150	20.87	20.77	1.56
I	731.1	200	19.25	19.24	c
I	36.1	10	19.27	19.25	1.51

TABLE 1B
OBSERVING LOG OF PHOTOGRAPHIC IMAGES

CTIO Number	Filter	Emulsion	Exposure (minutes)	$\mu_s(\text{Ap.})^d$ (mag s ⁻²)	Seeing
5309	GG 385	IIa-O	25	22.31	<1"
5316	GG 495	103a-D	12	21.15	<1"

^a Sky-normalized zero point based on aperture photometry.

^b Sky-normalized zero point based on standard stars.

^c This image showed slightly doubled star images due to an autoguider failure.

^d Based on an annular calibration (see text).

Inter-American Observatory are included in the analysis and provide a useful independent check on the CCD surface photometry. These plates also provide information on the outer parts of the galaxy not covered by the CCD images, at least in the *B* and *V* passbands.

The details of the CCD images and plates are compiled in Tables 1A and 1B, respectively. All images were normalized in the sky level, so that the zero points would equal the night sky brightness in mag arcsec⁻². Standard stars and aperture photometry were used to obtain zero points as in Papers I–III. Some of the aperture photometry used was taken from Longo & de Vaucouleurs (1983) and Lauberts & Sadler (1984), but in addition new photometry was obtained using the 0.9 m telescope of Cerro Tololo Inter-American Observatory and the 0.6 m telescope of Siding Spring Observatory (see Table 2). These observations were made using photometers with S-20 cathodes and standard filters. Although some of the *R* and *I* observations were made in the Johnson system, only those in the Cousins system were used in the present analysis. Table 1A also gives estimates of the seeing on each CCD image.

For the plates, the zero point calibration was more compli-

TABLE 2
APERTURE PHOTOMETRY OF NGC 7702

log <i>A</i> (0.1)	<i>V</i>	<i>B</i> – <i>V</i>	<i>U</i> – <i>B</i>	<i>V</i> – <i>R</i>	<i>R</i> – <i>I</i>	Red System ^a	Telescope ^b
0.63	13.17	1.00	0.61	0.57	0.63	KC	0.6 m
0.74	12.95	0.99	0.45	0.87	0.72	J	0.9 m
0.96	12.55	0.95	0.58	0.58	0.63	KC	0.6 m
1.04	12.48	0.94	0.53	0.87	...	J	0.9 m
1.04	12.44	0.95	0.46	0.86	...	J	0.9 m
1.12	12.36	0.94	0.58	0.6 m
1.22	12.29	0.94	0.44	0.84	0.71	J	0.9 m
1.34	12.24	0.93	0.47	0.90	0.51	J	0.9 m
1.34	12.21	0.93	0.41	0.84	...	J	0.9 m
1.42	12.16	0.93	0.42	0.6 m

^a KC = Kron-Cousins system; J = Johnson system.

^b 0.6 m at SSO; 0.9 m at CTIO.

cated. The core region was overexposed in both passbands, making it necessary to use an annular calibration to obtain zero points. The zero points in Table 1B were obtained by subtracting the flux in an aperture 25".6 in diameter from all successively larger apertures. A detailed comparison of surface photometry using elliptically averaged profiles is described in § 4.3.

In addition to the photometric information, long-slit spectra of NGC 7702 along the major and minor axes of the inner ring were obtained in 1981 July using the Ritchey-Chrétien image-tube spectrograph on the 4 m telescope of CTIO. These were exposed on preflashed, hypersensitized IIIa-J plates for 120 minutes along the major axis and 154 minutes along the minor axis, and cover a spectral range from near the Ca H and K lines to about 5600 Å. No absorption lines are detected in the ring, but, more importantly, neither is emission detected in the Balmer lines. The tentative implication is that the ring is purely stellar, although only four points in the ring were sampled.

3. MORPHOLOGY AND GROUP MEMBERSHIP

The *B* band CCD image of NGC 7702 is displayed in Figure 1 (Plate 9). The most conspicuous feature is the inner ring whose contrast is unusually high; it appears complete but is enhanced near its major axis. The image reveals a considerable amount of dust inside the ring on the near side, one lane of which actually crosses the ring. This is better illustrated in the *B*–*R* color index map displayed in Figure 2 (Plate 10), which also shows that the inner ring is a broad, subtle enhancement of bluer colors, especially near its major axis. The faint outer ring is only barely visible in Figures 1 and 2, but can be seen clearly on film copy J192 of the SRC Sky Survey.

NGC 7702 is an original Shapley & Ames (1932) galaxy and type estimates are given in several catalogs (see Table 3, where SGC = Corwin, de Vaucouleurs, & de Vaucouleurs 1985, RSA = Sandage & Tammann 1981, ESO-B = Lauberts 1982, and RC2 = de Vaucouleurs, de Vaucouleurs, & Corwin 1976). The four sources indicate a late S0 or S0/a classification, consistent with the previous three objects in this series.

The group membership of NGC 7702 was assessed using data in the Third Reference Catalogue of Bright Galaxies (RC3, de Vaucouleurs et al. 1990). Only two galaxies in the preliminary version of the catalog lie within 1° of NGC 7702. These, ESO 192-11 and ESO 192-12, have redshifts of 4700 and 10,350 km s⁻¹, respectively, compared to 3122 km s⁻¹ for NGC 7702 itself, and must be in the background. The only galaxies in the catalog having a similar redshift and which are within 6° of NGC 7702 are NGC 7650, NGC 7676, ESO 148-17, and NGC 7796. These have a mean redshift of 3310 km s⁻¹. However, all are more than 50 outer ring diameters away from NGC 7702.

4. DATA ANALYSIS

4.1. Integrated Properties

Basic integrated parameters of NGC 7702, calculated as in the previous papers in this series, are compiled in Table 3. Several of these parameters were also determined independently by Lauberts & Valentijn (1989) from an ESO-B plate, and the CCD data agree well with theirs. The distance of NGC 7702 is 29 Mpc if $H_0 = 100$ km s⁻¹ Mpc⁻¹ and if the velocity is reduced as described in Paper I. The absolute magnitude of the galaxy, after applying RC2 corrections to B_T in Table 3, is $M_T^2(B) = -19.8$.



FIG. 1.—B band CCD image of NGC 7702 (350 s exposure). This and Fig. 2 have north at the top and east to the left. The white bar is $20''$ in length. The image is logarithmic and the step scale ranges from $\mu_B = 28.0 \text{ mag arcsec}^{-2}$ (*darkest*) to $18.0 \text{ mag arcsec}^{-2}$ (*lightest*) in $1.0 \text{ mag arcsec}^{-2}$ steps.

BUTA (see 370, 131)

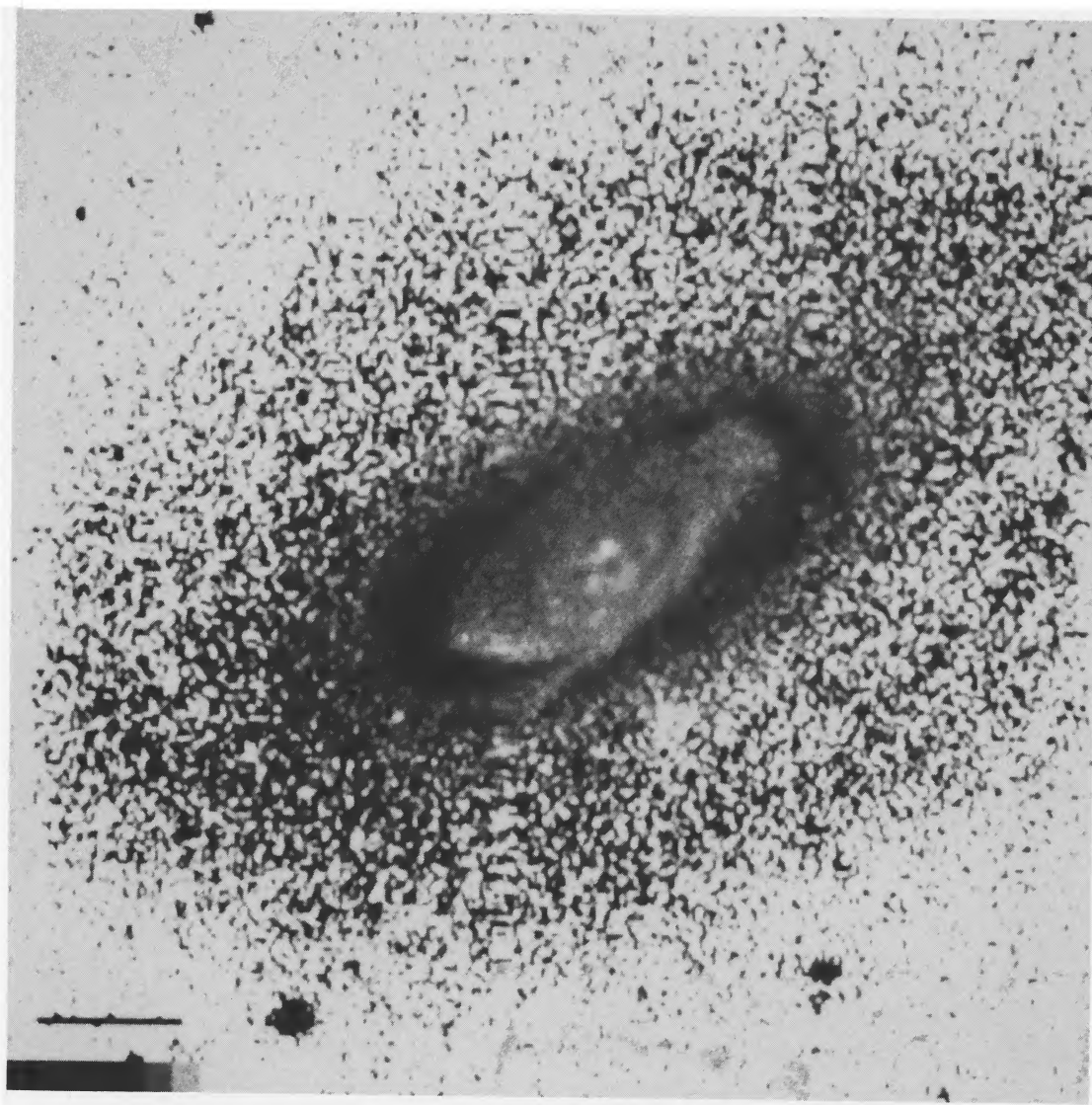


FIG 2.— $(B - R)$ color index map of NGC 7702. The dark horizontal bar is $20''$ in length. The step scale ranges from $B - R = 1.0$ (*darkest*) to 2.0 (*lightest*) in 0.1 mag steps.

BUTA (see 370, 131)

TABLE 3
BASIC AND INTEGRATED PARAMETERS^a

Parameter	Value	Parameter	Value
$\alpha(1950)$	23 ^h 32 ^m 44 ^s	$\log D_{25}$	1.335
$\delta(1950)$	-56°17'12"	$\log R_{25}$	0.331
l	323°1	$\theta_{25}(1950)$	122°
b	-58°1	$C_{21}(B)$	2.39
SGL	238°2	$C_{32}(B)$	1.69
SGB	-2°4	$r_1^*(B)$	0.13
ESO-B type	S0(r)	$r_2^*(B)$	0.30
SGC type	(R)SAB(r)0°	$r_3^*(B)$	0.51
RSA type	RSa(r)	$\mu_1(B)$	21.28 mag arcsec ⁻²
RC2 type	(R)SA(r)0 ⁺	$\mu_2(B)$	22.18 mag arcsec ⁻²
B_T	13.09 ± 0.04	$\mu_3(B)$	23.77 mag arcsec ⁻²
$\log A_e(B)$	0.81	$m_e'(B)$	12.60 mag arcmin ⁻²
$(B-V)_T$	0.92	$(B-V)_e$	0.98
$(U-B)_T$	0.42	$(U-B)_e$	0.50
$(V-R)_T$	0.57	$(V-R)_e$	0.56
$d(R)$	2.25 ± 0.10	$d(r)$	1.04 ± 0.03
$q(R)$	0.60 ± 0.04	$q(r)$	0.45 ± 0.01
i	57° ± 2°	$\theta(r)(1950)$	119° ± 1°
$\langle q(d) \rangle$	0.59 ± 0.01	$\theta(d)(1950)$	110° ± 2°
$\langle (U-B) \rangle(r)$	0.40 ± 0.03 (s.d.)	$\langle (B-V) \rangle(r)$	0.87 ± 0.04 (s.d.)
$\langle (V-R) \rangle(r)$	0.52 ± 0.03 (s.d.)	$\langle (V-I) \rangle(r)$	1.15 ± 0.06 (s.d.)

^a Positional information from Lauberts (1982) and RC3. A_e and D_{25} are in units of 0.1.

Integrated colors of NGC 7702 were obtained from the profiles in Figure 3, which are based on simulated aperture photometry using the CCD images only. These profiles also reflect the quality of the calibrations, since the zero points were directly determined from a fit of observed aperture photometry data to the simulated data, after applying transformation slopes determined from standard stars. The open circles refer to U measurements made with the 0.6 m SSO telescope (Table 2) in 1984. Three of these measurements are in systematic dis-

agreement with U measurements from other sources and were rejected from the zero point calculations.

Figure 3 also shows that the simulated run of $V-I$ with aperture size does not agree with available $V-I$ photoelectric measurements. This is mostly due to the I band surface photometry and is consistent with the findings in Paper III for NGC 7020, though there the effect was much worse.² The long-exposure I band image presented the most complex flat-field structure, fringing, the largest sky contribution, and suffered an autoguider failure and some core saturation. The systematic error may also in part be related to the steep gradient in the surface brightnesses at the center. It makes the I band surface brightnesses less precise than would be desired, but I believe they can still be used for structural studies.

4.2. Ring Shapes and Diameters

The dimensions of the inner ring were estimated by using a television display to define the ridge line of the color enhancement. An ellipse fitted to these points gave the diameter $d(r)$ and axis ratio $q(r)$ values in Table 3. The outer ring diameter $d(R)$ and axis ratio $q(R)$ are based instead on two independent visual estimates (de Vaucouleurs & Buta 1980a; SGC). The shapes of the two rings appear to be significantly different, and the ratio of their diameters, $d(R)/d(r) = 2.16$, is consistent with most double-ringed SB or SAB galaxies (Kormendy 1979; Athanassoula et al. 1982; Buta 1984, 1986a).

The intrinsic shape of the inner ring was estimated by assuming that isophotes beyond the outer ring characterize an axisymmetric disk. This disk has a mean axis ratio of 0.59 (§ 4.3), implying an inclination of about 57° if the intrinsic flattening is assumed to be 0.28 (Bottinelli et al. 1983). If we ignore the intrinsic thickness of the ring, then its approximate intrinsic axis ratio is $q_0(r) = 0.72$, far from circular.

If the distance to NGC 7702 is 29 Mpc, then the inner and outer rings are 8.8 and 19 kpc, respectively, in diameter. These

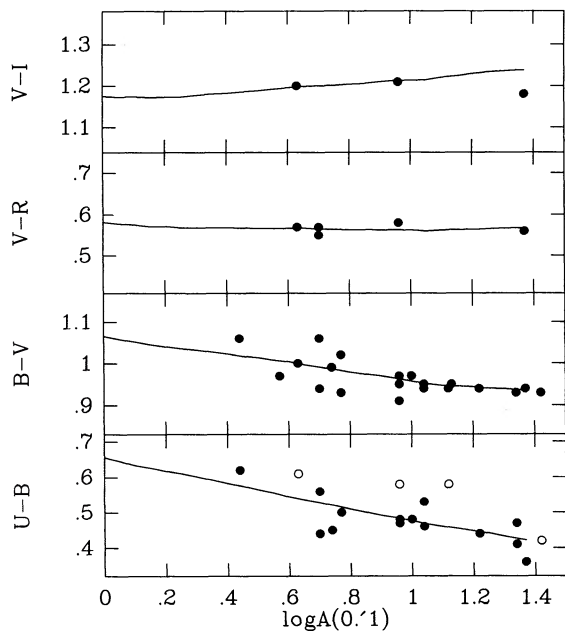


FIG. 3.—Color-aperture relations for NGC 7702. The solid curves are simulated from the surface photometry and take into account zero point and transformation relations based on standard stars and aperture photometry. The data points are available photoelectric measurements for comparison (see text).

² It was also present in the I band photometry of NGC 3081 (see Appendix A).

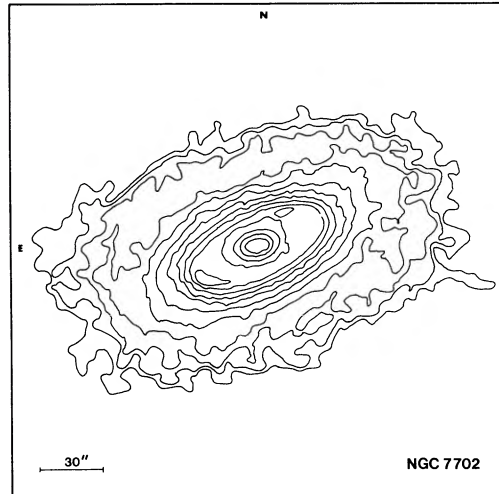


FIG. 4.—*B* band isophotes of the large-scale structure of NGC 7702, based on CTIO plate 5309 and the *B* band CCD image. The largest isophote is at $\mu_B = 27.0 \text{ mag arcsec}^{-2}$, and each successive isophote is separated by $-0.50 \text{ mag arcsec}^{-2}$. The isophotes were smoothed as follows: for $\mu_B > 22.0 \text{ mag arcsec}^{-2}$, a 5×5 Gaussian (weights from Jones et al. 1967; beam size = $3''.7$) was used; for $\mu_B \leq 22.0 \text{ mag arcsec}^{-2}$, a 3×3 boxcar average (box size = $1''.5$) was used.

are comparable to the sizes found for typical ringed SB galaxies (Buta & de Vaucouleurs 1982; Buta 1984).

4.3. Isophotes, Luminosity Profiles, and Disk Properties

Isophote maps of NGC 7702 are shown in Figures 4 and 5. The first is heavily smoothed in the outer parts and shows the large-scale structure to $\mu_B = 27.0 \text{ mag arcsec}^{-2}$; it is based on CTIO plate 5309 for $\mu_B > 22.0 \text{ mag arcsec}^{-2}$ and the *B* CCD image for $\mu_B \leq 22.0 \text{ mag arcsec}^{-2}$. The second is much less smoothed and is based on the short-exposure *I* band image; it prominently displays a small oval in the bulge region which has a major axis diameter of $8''$ (1.1 kpc) in a position angle of about 110° .

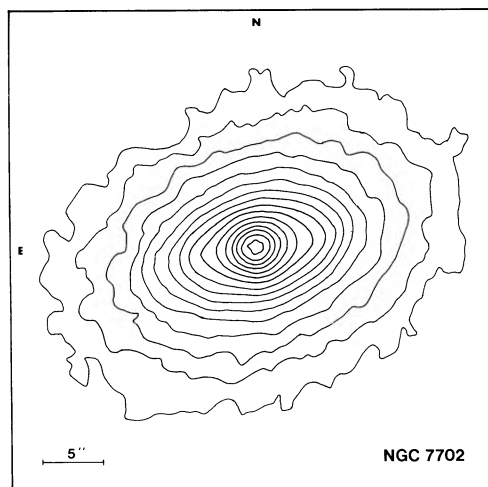


FIG. 5.—*I* band isophotes of the inner regions of NGC 7702, showing the nuclear oval. This is based on a 10 s *I* band CCD exposure. The largest isophote is at $\mu_I = 19.75 \text{ mag arcsec}^{-2}$, and each successive isophote is separated by $-0.25 \text{ mag arcsec}^{-2}$. The isophotes were smoothed using a 3×3 box average.

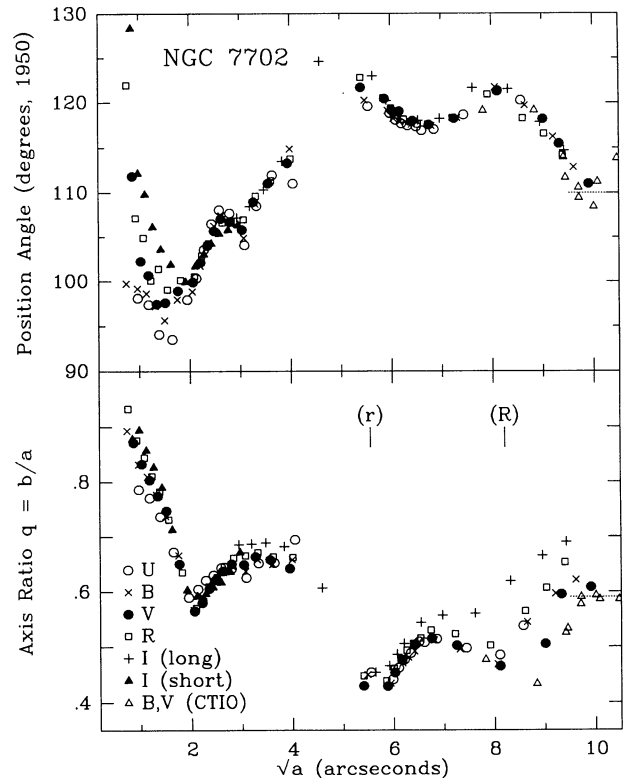


FIG. 6.—Dependence of isophote shapes and orientations on position within NGC 7702, based on ellipse fits. The legend at lower left identifies the filter associated with each symbol. The major axis positions of the inner ring (*r*) and outer ring (*R*) are indicated.

The radial dependences of the major axis position angle and shape of the isophotes are shown in Figure 6. The isophotes are nearly circular in the inner $1''$ but the axis ratios rapidly decrease to 0.59 at $a = 4''$. The position angle of the inner ring is 119° , but beyond this structure the position angle decreases to an uncertain limit of about 110° , which I tentatively adopt as the true major axis position angle. This latter estimate had to be based on the plates alone, because the important outer isophotes overflow the CCD images slightly; this probably explains the larger scatter in axis ratios for $a > 7''$. The mean disk axis ratio, $\langle q(d) \rangle$ in Table 3, also had to be based on the plates alone.

Figure 7 shows relative Fourier amplitudes of the deviations of the isophotes of NGC 7702 from elliptical shapes, based on the CCD images only. The amplitude A_4 is defined in Paper I, and it reveals significant 4θ deviations in the range $2'' \leq a \leq 6''$, with a maximum in all passbands near $a = 4''$. The sign of the $\cos 4\theta$ term is positive over this range in radius, consistent with the appearance of a pointed oval (as opposed to a rectangular oval). Higher order amplitudes (e.g., A_6) were found not to be significant.

Luminosity and color profiles along the major axis of the inner ring, based on the CCD images only, are shown in Figure 8. The *I* band profiles are based on a combination of the short- and long-exposure images, the former being used for the central few arcseconds. The contrast of the ring along the major axis is dependent on passband, being higher for *U* and *B*. The *U*–*R* color profile shows a dip along this axis at the ring position whose amplitude is a few tenths of a magnitude. The inner ring is much more subtle along the minor axis but is

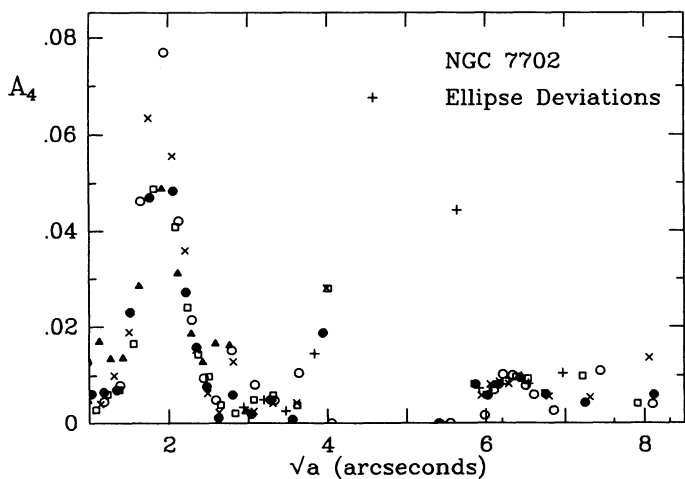


FIG. 7.—Relative amplitude of the 4th Fourier component for isophote ellipse deviations (see Fig. 6 for symbol legend). The major axis positions of the inner ring (r) and outer ring (R) are indicated.

still more of an enhancement in U and B than in V , R , and I . The outer ring along this axis has a surface brightness $\mu_B = 25.5 \text{ mag arcsec}^{-2}$, or 6% of the night sky brightness.

Both the CCD images and the photographic photometry were used to compute elliptically averaged profiles of NGC 7702, based on a disk axis ratio of 0.59 and a major axis position angle of 110° . A comparison between the resulting profiles for the B and V passbands revealed systematic differences larger than 0.2 mag in the inner $10''$, where the plates were overexposed (see § 2). Better agreement ($|\Delta\mu| \leq 0.05 \text{ mag}$) is found in the region of the inner ring ($r = 30''$), but between $40''$ and $80''$ the CCD surface brightnesses are systematically brighter than the photographic ones by up to -0.2 mag . The

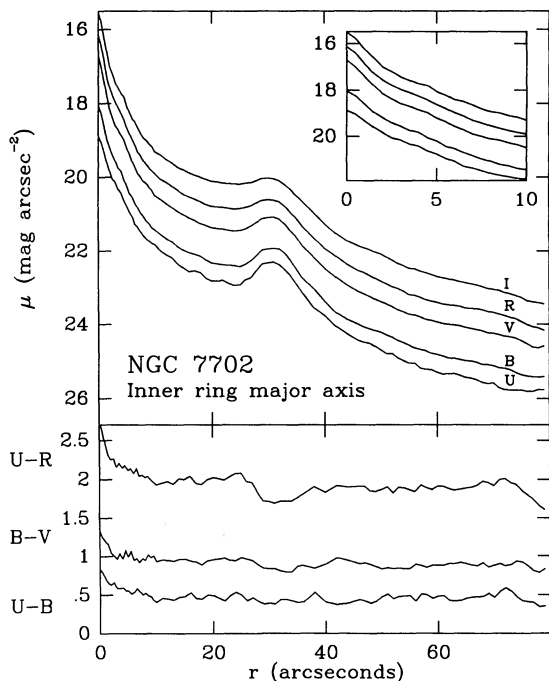


FIG. 8.—Surface brightness and color profiles along the major axis of the inner ring of NGC 7702, obtained by two-dimensional interpolation and based on CCD images only.

comparison is less reliable beyond $r = 80''$, because these radii overflow the CCD field and as a consequence the averages do not cover a full 360° .

The agreement between the CCD profiles and plate profiles is thus only fair, and the final B and V elliptically averaged profiles were constructed as follows: for $r < 40''$, the profiles are based on the CCD images alone; for $40'' \leq r < 80''$, the profiles are an average of the plate and CCD profiles; and for $r \geq 80''$, the profiles are based on the plates alone. For U , R , and I , the profiles are based on the CCD images only. Table 4 compiles the mean B band profile and several color index profiles, which are illustrated in Figure 9 (solid curves). Also shown are extended major and minor axis B band profiles (filled and open circles), the former of which is based on the B CCD image for $r < 76''$ and CTIO plate 5309 for $r \geq 76''$. The minor axis profile is based on the B CCD image alone. The elliptically averaged profile demonstrates that beyond $r = 80''$, the decline in surface brightness is approximately exponential. The extended major axis profile gives a consistent result, and the points (filled circles) shown for $r \geq 72''$ were used to obtain the scale length and central surface brightness of the exponential. The solution is

$$\mu_B = 20.943(\pm 0.160) + 0.059(\pm 0.002)r, \quad (1)$$

where r is in arcseconds. The data follow this relation reasonably well from $72''$ to $132''$, corresponding to only about 3.3 scale lengths. Using equation (8) of Simien & de Vaucouleurs (1986), the RC2 galactic extinction model, and $\log R_{2.5}$ from Table 3, then the corrected extrapolated central surface brightness is $B(0)_c = 21.5 \text{ mag arcsec}^{-2}$. This value agrees well with the Freeman (1970) mean value of 21.65.

The photometric properties of the bulge of NGC 7702 could

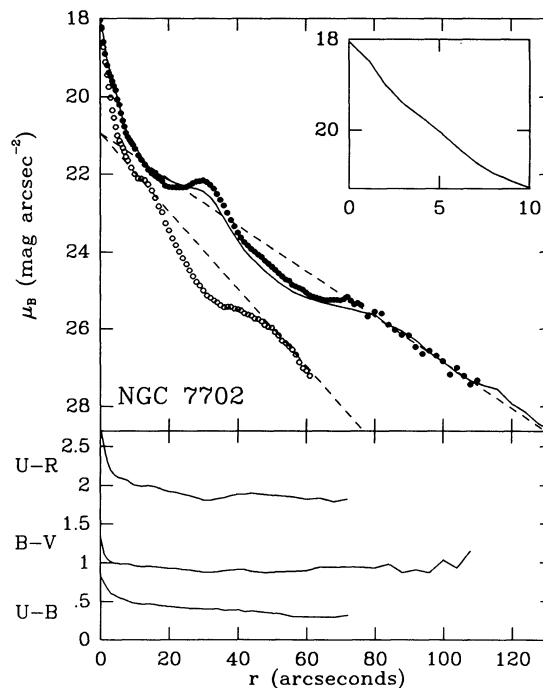


FIG. 9.—Azimuthally averaged surface brightness and color profiles (solid curves) of NGC 7702 for the disk major axis of 110° . Also displayed are a combined disk major axis B band profile (filled circles; see text) and the disk minor axis B band profile (p.a. = 20° , open circles). Dashed line for major axis is based on eq. (1); that for minor axis is inferred from disk axis ratio of 0.59.

TABLE 4
AZIMUTHALLY AVERAGED LUMINOSITY PROFILES OF NGC 7702^a

r	μ_B (mag arcsec ⁻²)	$B-V$	$U-B$	$V-R$	r	μ_B (mag arcsec ⁻²)	$B-V$	$U-B$	$V-R$
0"	18.05	1.34	0.83	0.58	40"	23.70	0.91	0.39	0.60
1	18.47	1.12	0.74	0.64	42	23.96	0.91	0.37	0.61
2	19.02	1.05	0.67	0.59	44	24.16	0.89	0.37	0.62
3	19.43	1.02	0.60	0.57	48	24.50	0.87	0.35	0.62
4	19.72	1.00	0.58	0.56	52	24.80	0.88	0.34	0.64
5	20.03	1.00	0.56	0.55	56	25.03	0.89	0.30	0.65
6	20.39	0.99	0.54	0.57	60	25.18	0.89	0.30	0.63
7	20.72	0.99	0.52	0.57	64	25.31	0.94	0.29	0.62
8	20.96	0.99	0.50	0.57	68	25.38	0.94	0.29	0.62
9	21.13	0.98	0.49	0.57	72	25.47	0.95	0.32	0.60
10	21.27	0.96	0.47	0.57	76	25.56	0.94	0.35	0.58
12	21.55	0.95	0.47	0.57	80	25.63	0.93
14	21.79	0.96	0.47	0.58	84	25.90	0.98
16	21.95	0.95	0.46	0.57	88	26.06	0.87
18	22.06	0.94	0.44	0.57	92	26.30	0.91
20	22.15	0.93	0.43	0.56	96	26.62	0.87
22	22.23	0.93	0.42	0.56	100	26.86	1.03
24	22.28	0.91	0.42	0.56	104	27.14	0.93
26	22.32	0.91	0.41	0.55	108	27.34	1.15
28	22.37	0.89	0.41	0.54	112	27.47
30	22.44	0.88	0.40	0.53	116	27.56
32	22.58	0.88	0.40	0.54	120	27.93
34	22.81	0.88	0.41	0.54	124	28.14
36	23.12	0.90	0.38	0.56	128	28.45
38	23.42	0.90	0.39	0.59	132	28.64

^a For disk major axis position angle of 110° and axis ratio of 0.59.

not be reliably obtained by any of the standard methods. The near side of the bulge is significantly affected by dust, and the parameters of a de Vaucouleurs $r^{1/4}$ law, even if present, can not be estimated reliably because of the small range in radius that would have to be used. The parameters would be too sensitive to the adopted seeing corrections. The method of Kent (1986) also cannot be used because the apparent flattening of the bulge is the same as that of the outer disk, with only a 10° difference in apparent position angle. Isophote shapes suggest that if the triaxial part of the bulge is embedded in a more ordinary spherical bulge (e.g., Kormendy 1982b), then this bulge is much fainter than the disk between the edge of the nuclear oval and the inner ring.

4.4. Relative Fourier Intensity Amplitudes

Relative Fourier intensity amplitudes for NGC 7702 in blue light are illustrated in Figure 10. These are based on a deprojection of the image and ignore finite thickness; only the first three even terms are shown because no odd terms or higher-order even terms were found to be significant by comparison. Radii are normalized to that of the $\mu_B = 25.0$ mag arcsec⁻² isophote ($r_{25} = 64''.9$). Only in the B band is the surface photometry reliable to well beyond the outer ring, thus allowing an assessment of the significance of a nonaxisymmetric component associated with the inner ring. For $r/r_{25} \leq 0.90$, the amplitudes are based on the B band CCD image, while for larger radii they are based on CTIO plate 5309. Ignoring the inner regions ($r/r_{25} < 0.2$), the analysis reveals significant $m = 2$ amplitude with a relatively constant phase over a large radius range around and beyond the inner ring. If we assume that the nonaxisymmetric component is characterized by the $m = 2$ and $m = 4$ components (e.g., Elmegreen & Elmegreen 1985; Buta 1986b; Ohta, Hamabe, & Wakamatsu 1990), then the integral of these components gives a fractional contribu-

tion of 14% within $r/r_{25} = 1.4$ with respect to the accumulated luminosity of the galaxy. Since the ring is largely stellar in nature, this implies that NGC 7702 may have an oval distortion which is bounded by the ring.

4.5. Ring Colors and Flux Contributions

The colors of the inner ring were measured in two ways. First, the ridge-line colors were measured by using a television display to define the ring's size and shape, and integrating the CCD fluxes at 33 positions within a circular aperture 4" in

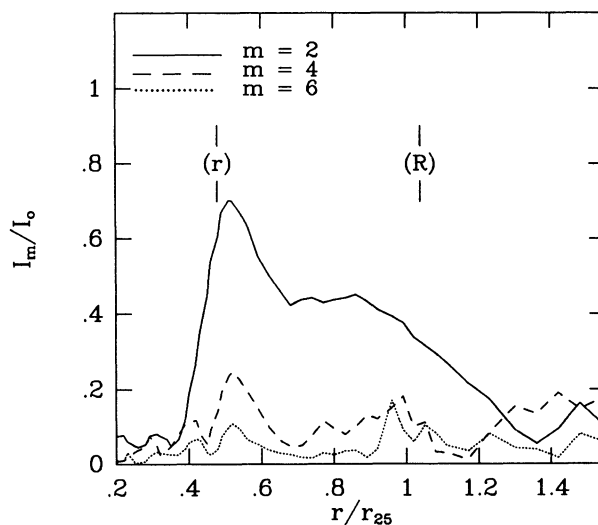


FIG. 10.—Relative Fourier intensity amplitudes (even terms only) for NGC 7702 in the B band. Radii are normalized to the $\mu_B = 25.0$ mag arcsec⁻² isophote.

diameter. The reddest colors are found on the south side where a dust lane crosses the ring, but the regions of the major axis are definitely enhanced with bluer colors. These regions are also sharply enhanced in surface brightness. Since NGC 7702 is highly inclined, these variations are probably not only due to some real changes in surface brightness and color around the ring, but also to dust and inclination (path length) effects as well as to the fact that a fixed size aperture was used for all ring points. The mean colors of the ring from this approach are compiled in Table 3.

In the second approach I compute azimuthally averaged profiles of NGC 7702 using elliptical annuli having the shape ($q = 0.45$) and orientation (p.a. = 119°) of the inner ring. This allows me to directly integrate the ring flux and at the same time make a correction for the "background," or underlying component of the ring (see Table 5). Only a simple method of background interpolation was used: linear fits were made to the surface brightnesses in the ranges $17''$ – $20''$ and $50''$ – $54''$, and these fits were interpolated under the ring hump. While this may give a reasonable estimate of the fluxes associated with the ring alone, we cannot be sure that the hump is not also due to a small amount of excess blue light superposed near the edge of a red lens. This is considered in the next section. The approach was initially applied for two radius ranges: $24'' \leq r \leq 38''$, corresponding to the width of the $U-R$ color dip along the major axis in Figure 8; and $20'' \leq r \leq 48''$, corresponding to the full ring/lens hump. However, since the results were found to be insensitive to the adopted radius range, Table 5 only gives the colors for the second radius range. The colors for the ring uncorrected for background agree well with the mean ring colors in Table 3, but the background-corrected colors are definitely bluer.

Table 5 also gives the colors of the inner ring hump corrected approximately for galactic and internal extinction and redshift. The corrections for U , B , and V followed RC2 procedures, while those for R and I were based on information given by Rieke & Lebofsky (1985) and Coleman, Wu, & Weedman (1980). The adopted corrections to the colors are $E(B-V) = 0.14$, $E(U-B) = 0.08$, $E(V-R) = 0.06$, and $E(V-I) = 0.13$. In interpreting the corrected colors, we have to keep in mind the uncertainties due to the background corrections, the bulge contribution, and the extinction corrections.

The evolution of the UBV colors of model galaxies with or without bursts is a problem which has been considered by Searle, Sargent, & Bagnuolo (1973) and Larson & Tinsley (1978, hereafter LT). A more recent study by Bica, Alloin, & Schmidt (1988) includes predicted $V-R$ and $V-I$ colors of star formation bursts superposed on old stellar populations;

TABLE 5
COLORS OF THE INNER RING HUMP AND BACKGROUND^a

Feature	$B-V$ ($B-V$) ₀	$U-B$ ($U-B$) ₀	$V-R$ ($V-R$) ₀	$V-I$ ($V-I$) ₀
(r) – background	0.79	0.35	0.44	0.92:
	0.65	0.27	0.38	0.79:
Background	0.94	0.44	0.59	1.30:
	0.80	0.36	0.53	1.17:
(r) + background	0.90	0.41	0.55	1.21:
	0.76	0.33	0.49	1.08:

^a These colors are based on a numerical integration of azimuthally averaged inner ring profiles within the radius range $20''$ – $48''$ (see text).

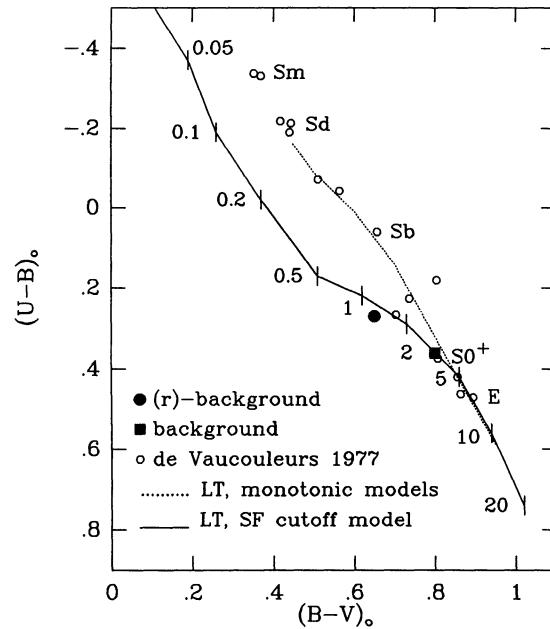


FIG. 11.—Color-color diagram for the background-corrected inner ring fluxes and the underlying ring background. Shown for comparison are mean integrated colors for normal galaxies from type E to Sm (open circles) and two model sequences from Larson & Tinsley (1978 = LT). Points on the curve for the star formation cutoff model are labeled by the age in units of 10^9 yr.

however, this work was designed more for comparison with starburst galactic nuclei rather than disk features such as a ring. Figure 11 shows how the background-corrected colors of the inner ring and the colors of the background alone compare with the mean integrated colors of galaxies of various types (de Vaucouleurs 1977) and two model sequences by LT: galaxies which have had a monotonically decreasing star formation rate during the past 10^{10} yr and galaxies which experienced a star formation cutoff after only 10^7 yr. This comparison shows that the colors of the background are relatively "normal" and are in fact very similar to the average integrated colors for $S0^+$ galaxies (calculated using the same kinds of corrections); however, the net colors of the ring are unusual and depart significantly from the integrated galaxy sequence. These colors instead are similar to those of the star formation cutoff model viewed at an age of 1 – 2×10^9 yr. Since the ring appears to lack any obvious H II regions or blue associations, then NGC 7702 provides an interesting possible example of a ring where star formation once was enhanced compared to its surroundings but has now either turned off or subsided to a low level. Refined burst models such as those in Figure 2 of LT and in Bica, Alloin, & Schmidt (1988) but which allow for the bluer color of the background disk population compared to E galaxy colors are needed before a more detailed interpretation of the colors of the ring can be made.

An important parameter relevant to a burst model of the ring is the burst strength, referring to the mass fraction of stars created in the burst relative to the total mass of the underlying galaxy (LT). Without knowledge of the mass-to-light ratio of the inner ring, we cannot estimate its mass fraction directly, but the ring major axis elliptically averaged profiles can be used to estimate the total apparent amounts of flux associated with the ring. Corrected for background, the relative contributions to the total luminosity are 11.7%, 11.3%, 10.4%, and

9.1% for the U , B , V , and R passbands, respectively.³ Restricting to the radius range occupied by the whole inner ring/lens hump, the relative contributions are more substantial, amounting to 45% in U , 42% in B , 37% in V , 32% in R , and 25% in I . If we assume that the net ring stellar population has $M/L_V \sim 0.75$ (interpolated from Table 1 of LT) and that the background galaxy has $M/L_V \sim 3$ (interpolated from Table 2 of LT), then the mass fraction of the ring relative to the galaxy could be only a few percent, while relative to its own radius range the mass fraction could be closer to 10%.

A reliable estimate of the luminosity fraction of the outer ring can only be obtained in blue light, and no serious correction for background can be made. Assuming that all light beyond $r = 60''$ is outer ring light, I find that it contributes only 12% of the total blue luminosity. Color profiles suggest that this feature is somewhat redder in $B-V$ than in the inner ring (see Table 4).

4.6. The Net Inner Ring Profile

The net luminosity profile of the inner ring was calculated from the folded ring major axis profiles displayed in Figure 8. As for the azimuthally averaged ring profiles described in the previous section, the background was interpolated linearly using the regions from $r = 17''-20''$ and $50''-54''$ to define the slope. The net inner ring profiles all could be fitted very well by the sum of two Gaussian components (see also Buta 1987): a narrow component having a dispersion of $\sigma_1 = 3''.6$ (0.51 kpc) and a broad component having $\sigma_2 = 6''.5$ (0.92 kpc). The average seeing over the five filters is only $\sigma^* = 0''.66 \pm 0''.04$, and so is not greatly affecting these results.

The fits also showed that the ratio of the peak intensity of the narrow component to the peak intensity of the broad component is a function of wavelength: $I_{0.1}/I_{0.2} = 1.70$ (U), 1.72 (B), 0.99 (V), 0.52 (R), and 0.20 (I); together with the dispersions, these ratios indicate that the narrow component is considerably bluer than the broad component. The mean radial position of each component was also found to be somewhat wavelength-dependent, ranging from $\langle r_1 \rangle = 30''.6-31''.1$ and $\langle r_2 \rangle = 32''.4-30''.7$ for filters U to I . The average radii over all five passbands were found to be identical, $\langle r_1 \rangle = \langle r_2 \rangle = 30''.9 \pm 0''.2$, implying that, within the errors of the fits, the two features overlap.

5. DISCUSSION

From the observations presented, we see that NGC 7702 is a complex ringed system that shares some properties in common with the other three objects in this series (NGC 3081, 7020, and 7187) as well as with ordinary ringed barred galaxies. The possibility that the galaxy owes its present structure to a collision or tidal interaction seems unlikely given its environment, which includes no companions of known similar redshift within about 50 outer ring diameters (~ 1 Mpc). The rings are therefore likely to have been generated by an internal perturbation, such as a bar or oval distortion. However, no n -body simulations have been successful in generating long-lived stellar rings in response to such perturbations (see, for example, Athanassoula 1983). Although a growing bar potential in a non-self-gravitating stellar disk or a static bar potential in a self-gravitating stellar disk might allow rings to form if models

could perhaps be carried over a sufficient number of bar rotations (see Elmegreen & Elmegreen 1985 and references therein), the simplest way to make rings seems to be in the response of gas to the forcing of a rotating bar (Schwarz 1979; Combes & Gerin 1985). The Schwarz models proved especially enlightening because they clarified a long suspected link between rings and resonances. Although van Albada (1985) has attributed the sharpness of the rings in Schwarz's models in part to his gas dissipation scheme, these models have nevertheless been successful in predicting many ring properties (e.g., Buta 1986a).

The Schwarz models suggest that an explanation for a galaxy like NGC 7702 may have to be sought in the secular evolution and depletion of a once gas-rich barred galaxy. The main lines of evidence to consider are (1) there is non-axisymmetry in the galaxy in the form of a triaxial bulge and an oval distortion, the latter of which must be bounded by the inner ring; (2) the inner ring is a zone of slightly enhanced blue colors compared to its surroundings; and (3) the size ratio of the inner and outer rings is consistent with what is observed for most other double-ringed barred galaxies. The triaxial bulge is perhaps the strongest piece of evidence that suggests that secular evolution has taken place in NGC 7702. This small feature alone cannot necessarily be regarded as an adequate explanation for the rings because it lies so far inside the rings. It is more likely that the nuclear bar of NGC 7702 is an analog of the nuclear bars of NGC 1291, NGC 1433, NGC 3081, and other galaxies in which a primary bar is more prominent (see, for example, Jarvis et al. 1988). Triaxial bulges in SB galaxies are believed to be a by-product of the ability of a bar to transport large amounts of gas into the centers of galaxies (Kormendy 1982b and references therein; Pfenniger & Norman 1990). This has been demonstrated both by n -body models and analytical models, and has found some observational support (Kormendy 1982b). The triaxial bulges usually show a large (sometimes perpendicular) angle with respect to a primary bar, which strongly suggests the influence of an inner Lindblad resonance (ILR) (Kormendy 1982b). The ILR has long been known to be a dissipative resonance (e.g., Lynden-Bell & Kalnajs 1972), and it may be possible for it to play a role in dissolving bars if the central mass concentration increases to the point where no orbits in the center support the bar (Hasan & Norman 1990). Since orbits inside the ILR of a galaxy with a high central density will be orthogonal to the primary bar axis, a triaxial bulge could be the remnant of a dissolved primary bar (Friedli & Pfenniger 1990).

If NGC 7702 once had a stronger, more important bar than it appears to have now, then it must also have had enough residual gas after it formed for long-term ring evolution. The original bar could have gathered gas into the two main rings via gravity torques acting on initially spiral shock fronts, as well as help to build up a high central concentration, making an ILR virtually unavoidable. The dissolution of the bar would not necessarily mean the demise of the rings, especially if these have been active star forming regions for a considerable fraction of the life-time of the galaxy. If rings are made of gas gathered into resonant periodic orbits, then the stars born in them will not necessarily leave the resonance region as they might leave spiral arms. Self-gravity could perhaps maintain the rings as the stars age. If star formation eventually ceases, as appears to be the case in NGC 7702, one would expect the ring to broaden with time (due to the expected increase in the velocity dispersion; see discussions in Mihalas & Binney [1981], Chap. 7.1, and Athanassoula [1983]), and therefore decrease in

³ This contribution is more difficult to estimate reliably for the I band with the present data owing to systematic errors in the surface brightnesses (§ 4.1), but the fraction presumably is similar to or slightly less than for the R band.

contrast. Inner and outer rings would be expected to evolve somewhat differently due to their different average positions in the galactic potential and presumably different velocity dispersions.

The results in § 4.6 can be used to evaluate these points to some extent. The Gaussian fits to the net inner ring profile indicate that the ring can be thought of as the sum of a narrow blue, possibly younger stellar population superposed on a broad, redder and presumably older stellar population. In the simplest interpretation, this is just what one would expect of an aging ring where enhanced star formation has proceeded over a considerable length of time. Stars born earlier in the ring would now populate a broader zone than initially, and being old they would likely be red. The narrow component would include the more recently formed stars which still lie near the narrower zone of gas compression. Even if star formation has completely ceased in the ring, one would expect to see both components provided the ring has existed for much of the lifetime of the galaxy. This has important implications for any burst interpretation of the net ring colors; as shown in § 4.5, these colors favor a limiting LT model where the duration of star formation in the burst was very short (10^7 yr). The current widths of the blue and red components would have to be tied intimately to the duration of the burst and its age, and it would seem that a longer burst duration might be required to explain the kind of net ring profile observed.

We can ask whether the current width of the ring is consistent with an age of 1.5×10^9 yr as suggested by its net colors. The radial velocity dispersion required to make stars born in the narrow shock zone of the ring spread out to a width of 510 pc during this time period is only $\sigma_v(r) \sim 0.33 \text{ km s}^{-1}$, much less even than the expected random velocities, 10 km s^{-1} , of interstellar gas clouds (see Mihalas & Binney 1981, p. 433). This discrepancy could possibly be explained by self-gravity of the ring, which could act to slow down the natural spreading tendency of the aging stars. It could also be due to the fact that the net ring hump does not entirely consist of stars born originally in the ring, especially if a bar once crossed the ring. That is, the lens may include stars which once belonged to the bar as well as old ring stars. If neither of these factors is important, then the ring would have to be considerably younger than 1.5×10^9 yr.

None of these arguments proves that NGC 7702 was once an SB spiral, since most published calculations suggest that even a mild oval distortion could be just as effective as an SB-type bar in generating rings and in secularly redistributing angular momentum (see Kormendy 1982 and references therein). This may be especially true if the oval has more mass than a typical SB-type bar, as might be suggested from the amount of light contained in the inner ring/lens of NGC 7702 (§ 4.4). However, as emphasized by Kormendy (1982b), triaxial bulges are most prominent in SB galaxies.

An important problem is the relationship between bars and ovals. Athanassoula (1983) has suggested that the difference between these structures lies in the initial velocity dispersion in the disk, hot disks favoring fat bars and cool disks favoring more elongated bars. In this picture, bars and ovals can be independent disk instabilities and one need not lead to the other. On the other hand, Kormendy (1979) suggested that when a bar dissolved, the end product could be a lens. The distinction between what Kormendy called an inner lens and what is generally recognized as an oval distortion is semantic in most cases, and the coexistence of bars and ovals in some

ringed galaxies (e.g., NGC 1433, Buta 1986b) suggests that secular evolution between bars and ovals may be important, although it is difficult to know how much the formation of a lens may also be tied to the evolution of a ring (Buta 1986b). Kormendy suggested the idea of bar dissolution because of the coincidence in sizes between bars and lenses, but another piece of evidence that would favor such a process would be to find galaxies which appear to be in a transitional state, that is, where a trace of the primary bar is still evident within an oval lens or ring. One such transitional case may be NGC 3081, as suggested by Kormendy (1979) and in Paper I. Since such cases seem to exist, it may not be unreasonable to consider NGC 7702 as an object in a more advanced state of morphological evolution.

In support of the above interpretations, I note that the size ratio of the rings of NGC 7702 is entirely consistent with that found on average for most barred galaxies having an inner and an outer ring (see § 4.2). This is unlikely to be a coincidence, and it suggests that the rings of NGC 7702 are associated with the same resonances believed to be responsible for inner and outer rings in barred galaxies, i.e., the inner 4:1 resonance and the outer Lindblad resonance, respectively (Schwarz 1979).

The structure of NGC 7702 therefore suggests that the galaxy may be a former barred spiral where not only the primary bar has dissolved, but star formation has also mostly ceased in the rings and in the center. The true nature of NGC 7702 may therefore be much more interesting than we can garner from surface photometry alone. Measurements of the rotation velocity and velocity dispersion from stellar absorption lines, accurate assessment of the stellar population of the inner ring (possibly from spectroscopic observations as well as photometry), and H I observations are needed for a better understanding of this enigmatic galaxy.

6. CONCLUSIONS

The main results of this paper are the following.

1. NGC 7702 is a genuine $S0^+$ galaxy with two rings, a bright inner ring of exceptionally high contrast, and a very low surface brightness outer ring of low contrast. The two rings have different shapes in projection, and if the inclination of the galaxy is characterized by the shape of the disk beyond the outer ring, then the inner ring has a significant intrinsic elongation compared to many SB inner rings.
2. Bulge isophotes reveal the presence of a small oval in the inner $4''$ radius. This oval shows significant $m = 4$ deviations from elliptical isophote shapes and is probably a nuclear bar. The feature is only one-eighth the diameter of the inner ring, and it seems unlikely (but not impossible) that it alone could have generated the stellar rings seen much farther out.
3. The inner ring is a slight blue enhancement compared to its surroundings. However, spectroscopic evidence reveals no sign of emission from the ring between the Ca H and K lines and the night sky 5577 \AA line, at least at four points along the major and minor axes, suggesting that the ring is purely stellar. The colors of the ring do not fit in with the notion of a feature which has had an enhanced, but continuously decreasing, rate of star formation since the galaxy formed. Instead, if the ring is defined as an excess of light above an exponentially decreasing background, then the net colors suggest that the ring experienced a burst of star formation less than 2×10^9 yr ago and has been evolving without much further activity ever since.
4. The net luminosity profile of the inner ring along its major axis is remarkably well fitted by the sum of two Gauss-

ian components, one red and one blue in color. The red component is nearly twice as broad as the blue component, but both components coincide nearly exactly in mean position. The two components can be easily understood in terms of an aging ring, but the broad component may not consist entirely of stars originally born in the ring.

5. The average luminosity distribution beyond the outer ring appears to follow an exponential law over a significant range. The extrapolated central surface brightness of this exponential is consistent with Freeman's well-known average for more normal spirals.

This series has presented photometric information on four extreme and mostly isolated examples of weakly barred early-type ringed disk galaxies. Each is a conspicuous double-ringed system, and each shows evidence for nonaxisymmetry either in the presence of nuclear bars or ovals, a low contrast normal bar, oval inner rings or lenses, or (in the case of NGC 7020), two blobs equidistant from the bulge. Are these non-axisymmetric components sufficient to explain the rings, which are mostly stellar in these early-type galaxies, or did some of these galaxies once have a stronger, more important bar which generated the rings when gas was more abundant and then mostly dissolved? The structure of each of these galaxies show

many properties in common with more obviously barred, ringed galaxies, but it is hard to understand why they have such high-contrast rings. Either strong, obvious bars are not required to form rings made largely of stars, or else bar dissolution is a real process that is going on in many galaxies. If the latter is correct, then important structures believed to be generated by bars, such as rings, can perhaps outlive the bars that created them. This is a problem requiring further research.

Note that of the four objects in this series, the most unique are NGC 7020 and NGC 7187. A fair number of other galaxies similar to NGC 3081 and NGC 7702 are included in the current version of the Catalogue of Southern Ringed Galaxies (Buta & Crocker 1990, in preparation; see Buta 1986a, 1990d) and in the catalogue of de Vaucouleurs & Buta (1980a). Several of these are NGC 2781, 2962, 3626, 3900, 4429, 4553, 6932, 7013, and 7742; a few will be described in a later paper.

I would like to thank G. de Vaucouleurs for initially bringing NGC 7702 to my attention during the early phases of my doctoral dissertation work. I would also like to thank Deborah A. Crocker and an anonymous referee for helpful comments on the manuscript.

APPENDIX

CORRECTIONS TO NGC 3081 PHOTOMETRY

New multiaperture photoelectric photometry of this galaxy, described in Paper I of this series, was obtained in 1990 March with the CTIO 1.0 m telescope and a GaAs phototube (Crocker & Buta 1990 and in preparation). This photometry indicates that corrections are required to the surface photometry in Paper I, as follows: $V-R = V-R(\text{Paper I}) - 0.04$; $V-I = V-I(\text{Paper I}) - 0.11$; and $B-I = B-I(\text{Paper I}) - 0.10$. The new photometry also revealed the existence of systematic errors in the I band photometry in Paper I that were not then recognized. These errors are similar to those found for NGC 7020 in Paper III. Systematic errors appear to be much less serious in the other filters.

REFERENCES

- Athanassoula, E. 1983, in *Internal Kinematics and Dynamics of Galaxies*, IAU Symposium 100, ed. E. Athanassoula (Dordrecht: Reidel), 243
- Athanassoula, E., Bosma, A., Creze, M., & Schwarz, M. P. 1982, *A&A*, 107, 101
- Bica, E., Alloin, D., & Schmidt, A. 1988, *A&A*, 242, 241
- Bottinelli, L., Gouguenheim, L., Paturel, G., & de Vaucouleurs, G. 1983, *A&A*, 118, 4
- Buta, R. 1984, Ph.D. thesis, University of Texas
- . 1986a, *ApJS*, 61, 609
- . 1986b, *ApJS*, 61, 631
- . 1987, *ApJS*, 64, 1
- . 1990a, *ApJ*, 351, 62 (Paper I)
- . 1990b, *ApJ*, 354, 428 (Paper II)
- . 1990c, *ApJ*, 356, 87 (Paper III)
- . 1990d, in *Dynamics of Galaxies and Molecular Clouds Distribution*, IAU Symposium 146, ed. F. Combes & F. Casoli (New York: Kluwer), in preparation
- Buta, R., & de Vaucouleurs, G. 1982, *ApJS*, 48, 219
- Coleman, G. D., Wu, C.-C., & Weedman, D. W. 1980, *ApJS*, 43, 393
- Combes, F., & Gerin, M. 1985, *A&A*, 150, 327
- Corwin, H. G., de Vaucouleurs, A., & de Vaucouleurs, G. 1985, *Southern Galaxy Catalogue* (Austin: University of Texas Monograph No. 4) (SGC)
- Crocker, D. A., & Buta, R. 1990, in *Dynamics of Galaxies and Molecular Clouds Distribution*, IAU Symposium 146, ed. F. Combes & F. Casoli (New York: Kluwer), in preparation
- de Vaucouleurs, G. 1977, in *The Evolution of Galaxies and Stellar Populations*, ed. B. Tinsley & R. Larson (New Haven: Yale University Observatory), 43
- de Vaucouleurs, G., & Buta, R. 1980a, *AJ*, 85, 637
- . 1980b, *ApJS*, 44, 451
- de Vaucouleurs, G., de Vaucouleurs, A., & Corwin, H. 1976, *Second Reference Catalogue of Bright Galaxies* (Austin: University of Texas Press) (RC2)
- de Vaucouleurs, G., de Vaucouleurs, A., Corwin, H., Buta, R., Paturel, G., & Fouque, P. 1990, *Third Reference Catalogue of Bright Galaxies* (New York: Springer)
- Dressler, A. 1984, *ARAA*, 22, 185
- Elmegreen, B. G., & Elmegreen, D. M. 1985, *ApJ*, 288, 438
- Freeman, K. C. 1970, *ApJ*, 160, 811
- Friedli, D., & Pfenniger, D. 1990, in *Dynamics of Galaxies and Molecular Clouds Distribution*, IAU Symposium 146, ed. F. Combes & F. Casoli (New York: Kluwer), in preparation
- Gregg, M. 1989a, *ApJS*, 69, 217
- . 1989b, *ApJ*, 337, 45
- Hasan, H., & Norman, C. 1990, *ApJ*, 361, 69
- Jarvis, B. J., Dubath, P., Martinet, L., & Bacon, R. 1988, *A&AS*, 74, 513
- Jones, W., Obits, D., Gallet, R., & de Vaucouleurs, G. 1967, *Astronomical Surface Photometry by Numerical Mapping Techniques* (Austin: Pub. Dept. Astr. Univ. Texas, 2d Ser., Vol. 1, No. 8)
- Kent, S. M. 1986, *AJ*, 91, 1301
- Kormendy, J. 1979, *ApJ*, 227, 714
- . 1982a, in *Morphology and Dynamics of Galaxies* (Geneva: Geneva Observatory), 115
- . 1982b, *ApJ*, 257, 75
- Larson, R. B., & Tinsley, B. M. 1978, *ApJ*, 219, 46 (LT)
- Lauberts, A. 1982, *The ESO-Uppsala Survey of the ESO (B) Atlas* (Munich: European Southern Observatory) (ESOB)
- Lauberts, A., & Sadler, E. M. 1984, *ESO Sci. Rept.*, No. 3
- Lauberts, A., & Valentijn, E. A. 1989, *The Surface Photometry Catalogue of the ESO-Uppsala Galaxies* (Munich: European Southern Observatory)
- Longo, G., & de Vaucouleurs, A. 1983, *A General Catalogue of Photoelectric Magnitudes and Colors in the U, B, V System of 3,578 Galaxies Brighter than the Sixteenth V-Magnitude* (Austin: Univ. Texas Monog. Astr., No. 3)
- Lynden-Bell, D., & Kalnajs, A. 1972, *MNRAS*, 157, 1
- Mihalas, D., & Binney, J. 1981, *Galactic Astronomy* (New York: Freeman)
- Ohta, K., Hamabe, M., & Wakamatsu, K. 1990, *ApJ*, 357, 71
- Pfenniger, D., & Norman, C. 1990, *ApJ*, 363, 391
- Rieke, G. H., & Lebofsky, M. J. 1985, *ApJ*, 288, 618
- Sandage, A., & Tammann, G. A. 1981, *A Revised Shapley-Ames Catalogue of Bright Galaxies* (Washington: Carnegie Institution of Publication No. 635) (RSA)
- Schwarz, M. P. 1979, Ph.D. thesis, Australian National University
- Searle, L., Sargent, W., & Bagnuolo, W. 1973, *ApJ*, 179, 427
- Shapley, H., & Ames, A. 1932, *Harvard Obs. Annals*, No. 2
- Simien, F., & de Vaucouleurs, G. 1986, *ApJ*, 302, 564
- van Albada, G. 1985, *A&A*, 142, 491
- van Driel, W. 1987, Ph.D. thesis, University of Groningen